7-3

A technique for phase-detection auto focus under near-infrared-ray incidence in a back-side illuminated CMOS image sensor pixel with selectively grown germanium on silicon

Tatsuya Kunikiyo, Hidenori Sato, Takeshi Kamino, Koji Iizuka, Ken'ichiro Sonoda and Tomohiro Yamashita
Renesas Electronics Corporation, 751 Horiguchi, Hitachinaka, Ibaraki, 312-8504, Japan.
Corresponding author: tatsuya.kunikiyo.zn@renesas.com

***Abstract*—A novel phase-detection auto focus (PDAF) technique for incident 850 nm plane wave is demonstrated using Ge-on-Si layer and deep trench isolation (DTI), which are locally arranged on light receiving surface (LRS) of crystalline silicon (c-Si). No metal light shielding film (LSF) for pupil division is formed. The key concept of the present work for PDAF is to perform the pupil division by the locally arranged Ge-on-Si layer in a pixel according to incident angle. The present pixel is based on a back-side illuminated CMOS image sensor pixel; the pixel pitch is 1.85 μm and the thickness of c-Si is around 3 μm. The simulation, based on three-dimensional finite difference time domain (3D-FDTD) method, shows that the external quantum efficiency (EQE) of the present pixel exhibits above 44.3 % with the maximum of 76.0 % for incident angles of -30° to +30°, owing to the selectively arranged Ge-on-Si layer; it exhibits 3.6 times improvement in the EQE at normal incidence compared to that of current state-of-the-art pixel with half metal-shielded aperture; the EQE is 49.2 % and 13.8 %, respectively. The present technique can enhance the accuracy of AF under low-illuminated condition.**

I. INTRODUCTION

The demand for auto focus in night vision photography requires a technique for phase-detection auto focus (PDAF) to capture near infrared radiation. To achieve a high accuracy of PDAF under low-illuminated condition, it is desired to increase external quantum efficiency (EQE) in a pixel for PDAF fabricated on a cost-effective crystalline silicon (c-Si) substrate.

The PDAF method in digital cameras is a system to which so-called triangulation technique is applied and is a method of obtaining a distance by an angle difference when seeing the same subject from two different points. In a pixel for PDAF, a light shielding film (LSF) for limiting light incident on the micro lens is provided [1], and the amount of light incident on the image pickup element is limited, so that the sensitivity is deteriorated. As a result, there is a possibility that accuracy of detection of the focal position may be lowered.

Moreover, absorption coefficient in c-Si at wavelength of 850 nm is almost one order of magnitude smaller than that at wavelength of 550 nm [2]. While it is possible to obtain a higher EQE by simply having a thicker c-Si absorption layer, the resultant higher power supply voltage for charge transfer may increase power consumption; therefore, it is challenging to design a high-performance silicon pixel for PDAF under near-infrared-ray incidence.

II. PUPIL DIVISION DUE TO GE-ON-SI LAYER

The key concept of the present study for PDAF is to realize pupil division by the Ge-on-Si layer [3][4] selectively grown on the light-receiving surface (LRS) of c-Si, as shown in Fig. 1 and Table 1; the key concept utilizes the characteristic that absorption coefficient of germanium is much larger than that of silicon. Due to the ~0.8 eV direct bandgap of Ge, compared to Si, a stronger absorption manifests itself with cut-off wavelength up to 1.6 μm. The Ge film thickness required for a strong interaction with near infrared light is usually more than 200 nm [3]; therefore, the Ge film thickness is set to 200 nm in the present study.

The present pixel is based on a back-side illuminated CMOS image sensor pixel with one photo diode for visible light. The pixel pitch is 1.85 μm and the thickness of c-Si is around 3 μm. In order to suppress crosstalk, a deep trench isolation (DTI) is provided on the pixel boundary. The Ge-on-Si layer is formed by anisotropically etching the c-Si on the LRS to depth of 200 nm and then filling the trench with a crystalline Ge layer so that the Si and Ge layers on the LRS become uniform.

Table 1 summarizes the investigated pixels for PDAF. In the proposed pixel A with a red color filter (CF), we have placed the Ge-on-Si layer selectively so that light with incident angles of +0° to +30° strikes the Ge-on-Si layer. Moreover, we have formed no metal LSF for pupil division, which avoids flare and ghost arising from the LSF; therefore, the present technique is different from the prior art categorized into three types: half-shielding pixel [1], one pixel having two photo diodes [5] and two pixels sharing a micro lens [6].

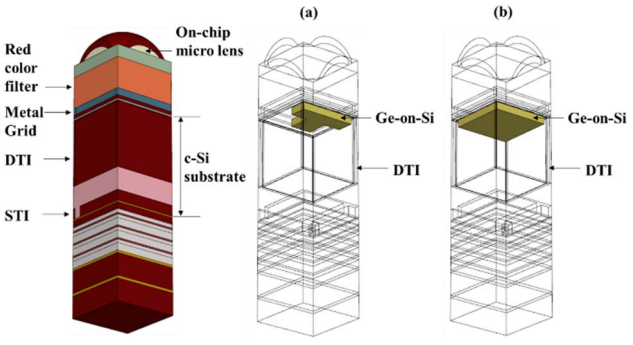

Figure 1. View from below of the present pixel for PDAF. Only the Ge-on-Si layer in (a) pixel A and (b) B (shown in Table 1) are displayed, respectively.

Table 1. Investigated pixels for PDAF.

pixel name		Cross section at metal grid	Cross section at light receiving surface
A	Ge-on-Si arranged in the shape of T w/o LSF (proposed)	Red Color filter, Metal grid	Crystalline silicon, Ge-on-Si, DTI, unit: μm
B	Ge-on-Si w/ LSF	Light shielding film (LSF)	Ge-on-Si, DTI, unit: μm
C	No Ge-on-Si w/ LSF (reference)	Light shielding film (LSF)	Crystalline silicon, No DTI
D	No Ge-on-Si w/o LSF (adjacent to the left side of the pixel A)	Green Color filter, Metal grid	Crystalline silicon, DTI
E	Same as Pixel A except Ge-on-Si layer	Red Color filter, Metal grid	Crystalline silicon, DTI

The proposed pixel A has neither a metal grid (MG) nor a DTI at the boundary with an adjacent pixel on the left; we omitted them to enhance EQE at an incident angle of +30°. The configuration of the pixels adjacent to the pixel A is the same except the on-chip CF; the DTI and MG of the adjacent pixels are arranged symmetrically with the pixel A in the Bayer format, but the no Ge-on-Si are placed, shown as pixel D in Table 1. The pixel D with the on-chip green CF is used for correcting EQE ratio and contrast of the pixel A, which are relevant to the accuracy of AF.

In the pixel B with half metal-shielded aperture, the Ge-on-Si is grown to cover most region of the LRS. Reference pixel C is a current state-of-the-art pixel for PDAF [1]. The pixel E is same as the pixel A except for the Ge-on-Si layer.

III. Results and Discussion

We calculated the optical wave propagation in the pixels by rigorously solving the Maxwell's equations, using a three-dimensional finite difference time domain (FDTD) algorithm [7]; we considered both TE- and TM-polarized light and set the periodic boundary condition corresponding to the Bayer format.

Figure 2 displays simulated angular response of power flux density distribution in the pixels (a) A and (b) C, respectively: the distribution under the propagation of TM-polarized light at the wavelength of 850 nm. Fig. 2 (c) illustrates the direction of TM polarization at normal incidence (+0°) for upper figures of Fig. 2 (a) and (b).

In the pixel A, when the incident angle is +10° to +30°, the incident light is absorbed mainly by the Ge-on-Si layer, and the light passing through the Ge-on-Si layer is attenuated and distributed in the Si layer; the pixel A exhibits smaller spread of the distribution for the same incident angles in comparison with the reference pixel C with the half metal-shielded aperture; this is remarkable in the comparison of power flux density distribution in LRS. The light transmitted to the wiring layer of the pixel A is smaller than that of the pixel C for the incident angle of 0° to +20°.

Figure 3 shows that the simulated angular response of the EQE behaves differently depending on the polarization; in the pixel E, reflection occurs on the sidewall of the MG for incident angles of +20° to +30°, so the difference in the EQE due to the polarization is clearly observed: the closer the angle of incidence on the sidewall approaches the Brewster angle, the greater the difference in the EQE due to the

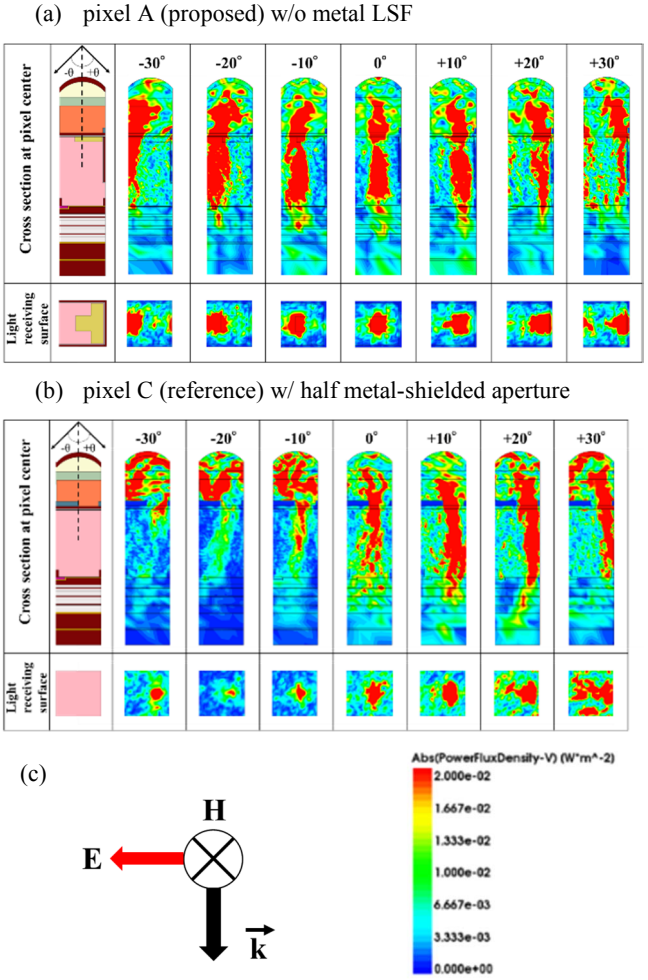

Figure 2. Simulated angular response of power flux density distribution by the propagation of TM-polarized light at wavelength of 850 nm in the cross section at the pixel center (upper figure) and at the light receiving surface (lower figure) of (a) the proposed pixel A, (b) the reference pixel C, respectively; (c) direction of TM polarization at normal incidence (+ 0°) for upper figures

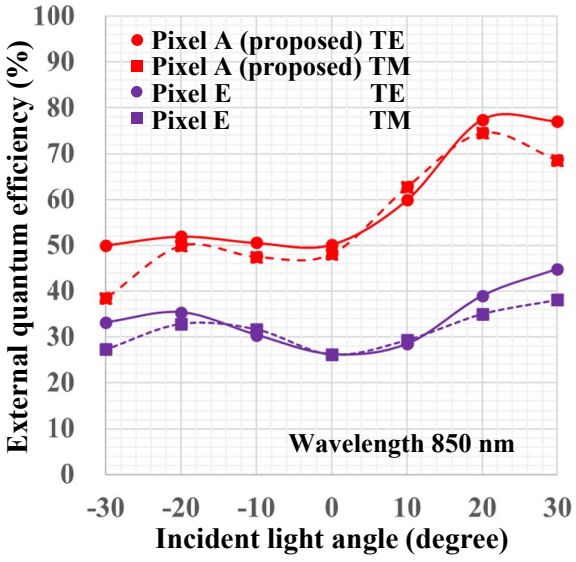

Figure 3. Simulated angular response of external quantum efficiency at wavelength of 850 nm.

polarization. Thus, the average values of the EQE by the propagation of TE- and TM-polarized light for each incident angle are used in the following graphs for simplicity.

Figure 4 displays simulated angular response of the EQE for the pixels shown in Table 1. The EQE of the proposed pixel A exhibits above 44.3 % with the maximum of 76.0 %. The EQE increases from the incident angle of +0° to +30° because the light hits the Ge-on-Si layer and is absorbed.

On the other hand, the reference pixel C exhibits the EQE of 4.9 to 23.0 %. The pixel A exhibits 3.6 times improvement in the EQE at normal incidence (+0°) compared to that of the pixel C; the EQE is 49.2 % and 13.8 %, respectively. The EQE in the pixel B is higher by 5.6 to 22.5 points compared to that in the reference pixel C because of the Ge-on-Si layer.

Even though half of the pixels are shielded by a metal film, the EQE of pixels B and C is larger than 10.5 % and 4.9 %, respectively, at incident angle of -30° to -10°; this is due to light diffraction.

The EQE of the pixel D is lower than that of the pixel E due to the difference in color filters. The curve of the EQE of the pixel E is smallest at the incident angle of 0° because the optical path length in the c-Si layer is the shortest.

The difference in EQE of the pixel E at the incident angle of ±30° is due to the presence or absence of DTI at the pixel boundary; it is suggested that the crosstalk to the adjacent pixels is different. The same is true for the pixel D.

Figure 5 shows the curves of the EQE gain by the selectively arranged Ge-on-Si layer; the EQE gain was calculated by taking the difference between the EQEs of pixels (A and D) or (A and E). The difference in the EQE between pixels A and D shows the EQE gains of 29.6 to 56.5 points for incident angles of +0° to +30°. On the other hand, the difference in the EQE between pixels A and E shows the EQE gains of 23.0 to 39.0 points for incident angles of +0° to +30°.

In addition, the curves of the EQE gain behave in the same manner as the EQE curve of the reference pixel C; they behave similarly to the reference curve in that the curve from the incident angle of -20° to +20° increases monotonically. Therefore, that has numerically confirmed the validity of the pupil division due to the selectively arranged Ge-on-Si layer and the differential operation.

Furthermore, the characteristic curves of EQE gain show EQE values higher than that of the reference pixel C. This suggests that the pupil division works effectively even in a dark environment where the reference pixel C does not operate.

Figure 6 displays simulated EQE as a function of reflectance. In this figure, the horizontal axis of Fig. 4 is changed from the incident angle to the reflectance; the purpose is to clarify the influence of the reflectivity of the Ge-on-Si layer on the EQE.

The optical reflection loss in the pixels A, D and E with no LSF is below 24.0 %; and the EQE of those pixels is more than 16.4 %. The EQE of the pixel A with the Ge-on-Si layer is higher than that of the pixel E despite a slightly higher reflectance on average; therefore, the selectively arranged Ge-on-Si layer is the main factor for the EQE enhancement. The same is true for the comparison of the pixels B and C which have half metal-shielded aperture.

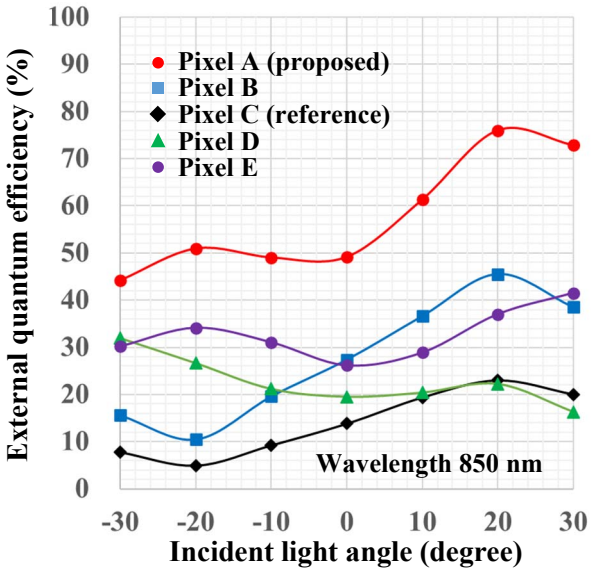

Figure 4. Simulated angular response of external quantum efficiency at wavelength of 850 nm.

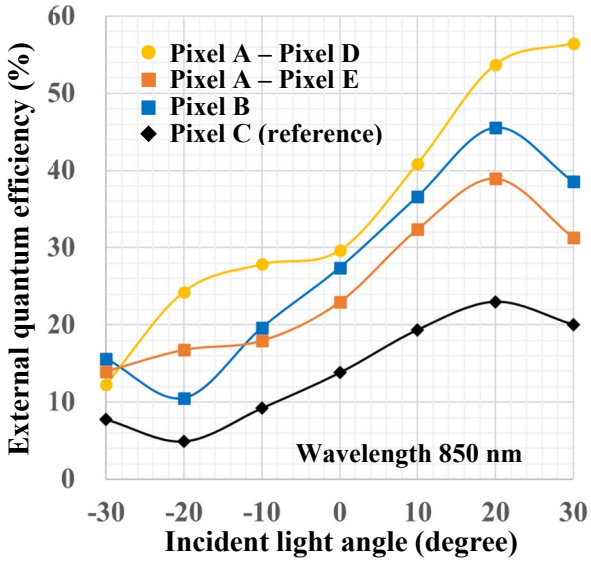

Figure 5. Evaluation of the simulated EQE gain due to the Ge-on-Si layer.

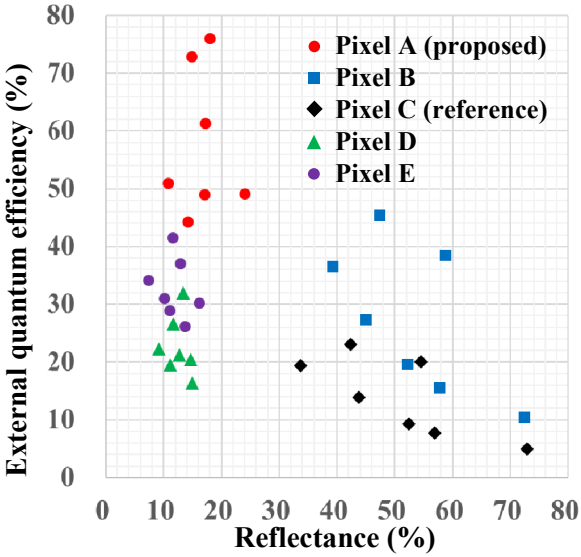

Figure 6. Simulated effective quantum efficiency as a function of reflectance at wavelength of 850 nm.

Figures 7 and 8 show simulated angular response of normalized EQE ratio and the Michaelson contrast, respectively. The Michaelson contrast is defined by the following equation:

$$\text{Michaelson contrast} = \left| \frac{\Psi_{+\theta} - \Psi_{-\theta}}{\Psi_{+\theta} + \Psi_{-\theta}} \right|$$

$\Psi_{+\theta}$: EQE at incident light angle $+\theta$

$\Psi_{-\theta}$: EQE at incident light angle $-\theta$

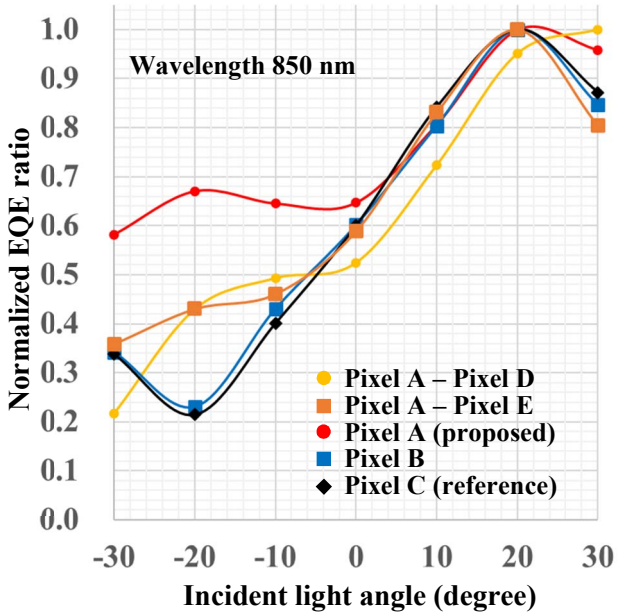

Figure 7. Simulated angular response of normalized external quantum efficiency ratio at wavelength of 850 nm.

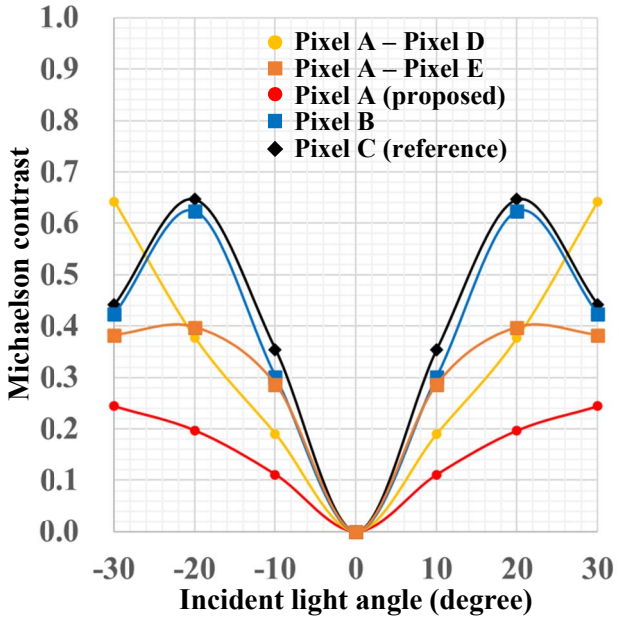

Figure 8. Simulated angular response of Michaelson contrast at wavelength of 850 nm.

The characteristics of the EQE ratio and the contrast of the pixel A deviates from those of the reference pixel C; especially, there is a deviation in the curve from the incident angle of -30° to -10°. This is because there is no light-shielding film that covers half the pixels. To correct the deviation, the EQE ratio and the contrast subjected to the same differential operation as that in Fig. 5 were executed. By taking the difference, the characteristic curve of the EQE gain due to the Ge-on-Si layer locally formed on the LRS can be obtained. The curves based on the difference operation behave in the same manner as the reference curves, showing that the same effect as the pupil division by LSF is obtained by the selectively arranged Ge-on-Si layer and the differential operation.

Conclusions

A novel PDAF technique for incident 850 nm plane wave is demonstrated using the Ge-on-Si layer, which are locally arranged on light receiving surface (LRS) of crystalline silicon (c-Si). No metal light shielding film for pupil division is formed. The key concept of the present study for PDAF is to perform the pupil division by the locally arranged Ge-on-Si layer in a pixel according to incident angle. The present pixel is based on a back-side illuminated CMOS image sensor pixel; the pixel pitch is 1.85 μm and the thickness of c-Si is around 3 μm. The simulation, based on three-dimensional finite difference time domain (3D-FDTD) method, shows that the external quantum efficiency (EQE) of the present pixel exhibits above 44.3 % with the maximum of 76.0 % for incident angles of -30° to +30°, owing to the selectively arranged Ge-on-Si layer; it exhibits 3.6 times improvement in the EQE at normal incidence compared to that of current state-of-the-art pixel with half metal-shielded aperture; the EQE is 49.2 % and 13.8 %, respectively. By taking the difference from the EQE of the similar pixel except for the Ge-on-Si layer, the characteristic curve of the present pixel behaves in the same manner as that of the current state-of-the-art pixel; therefore, that has numerically confirmed the validity of the pupil division due to the selectively arranged Ge-on-Si layer and the differential operation.

References

[1] R. Fontaine, "The State-of-the-Art of Mainstream CMOS Image Sensors," Proc. of International Image Sensor Workshop (IISW), 2015.

[2] M. A. Green, "Self-consistent optical parameters of intrinsic silicon at 300 K including temperature coefficients", Solar Energy Materials and Solar Cells, vol. 92, pp. 1305–1310, 2008.

[3] J. Michel, J. Liu, L. C. Kimerling, "High-performance Ge-on-Si photodetectors," Nature Photonics, 4, pp. 527-534, 2010.

[4] N. Na, S.-L. Cheng, H.-D. Liu, M.-J. Yang, C.-Y. Chen, H.-W. Chen, Y.-T. Chou, C.-T. Lin, W.-H. Liu, C.-F. Liang, C.-L. Chen, S.-W. Chu, B.-J. Chen, Y.-F. Lyu, S.-L. Chen, "High-Performance Germanium-on-Silicon Lock-in Pixels for Indirect Time-of-Flight Applications," Tech. Dig. of IEEE International Electron Devices Meeting (IEDM), pp. 751-754, 2018.

[5] M. Kobayashi, M. Johnson, Y. Wada, H. Tsuboi, H. Takada, K. Togo, T. Kishi, H. Takahashi, T. Ichikawa, S. Inoue, "A Low Noise and High Sensitivity Image Sensor with Imaging and Phase-Difference Detection AF in All Pixels," ITE Trans. on Media Technology and Applications (MTA), Vol.4, No. 2, pp. 123-128, 2016.

[6] WIPO Pub. No. WO2016/09864.

[7] Synopsys, 2016.